Analyst

Synthesis of highly dispersive sinapinic acid@graphene oxide (SA@GO) and their applications as a novel surface assisted laser desorption/ionization mass spectrometry for proteomics and pathogenic bacteria biosensing

Journal:	*Analyst*
Manuscript ID:	AN-ART-11-2014-002158
Article Type:	Paper
Date Submitted by the Author:	23-Nov-2014
Complete List of Authors:	Abdelhamid, Hani; NSYSU, chemistry department Wu, Hui Fen; National Sun Yat-Sen University,

Synthesis of highly dispersive sinapinic acid@graphene oxide (SA@GO) and their applications as a novel surface assisted laser desorption/ionization mass spectrometry for proteomics and pathogenic bacteria biosensing

Hani Nasser Abdelhamid [1,2], Hui-Fen Wu[1,3,4,5,6]**

[1]Department of Chemistry, National Sun Yat-Sen University, Kaohsiung, 804, Taiwan
[2]Department of Chemistry, Assuit University, Assuit, 71515, Egypt
[3]School of Pharmacy, College of Pharmacy, Kaohsiung Medical University, Kaohsiung, 800, Taiwan
[4]Center for Nanoscience and Nanotechnology, National Sun Yat-Sen University, Kaohsiung, 804, Taiwan
[5]Doctoral Degree Program in Marine Biotechnology, National Sun Yat-Sen University and Academia Sinica, Kaohsiung, 804, Taiwan
[6]Medical Science and Technology, National Sun Yat-Sen University, Kaohsiung, 804, Taiwan
*Corresponding author. Tel: 886-7-5252000-3955. Fax: 886-7-525-3908.
E-mail: hwu@faculty.nsysu.edu.tw (Prof. Hui-Fen Wu)

Abstract

Graphene oxide (GO) modified sinapinic acid (3,5-dimethoxy-4-hydroxy cinnamic acid, SA) (SA@GO) was synthesized, characterized and it was investigated as a new surface assisted laser desorption/ionization mass spectrometry (SALDI-MS) for proteomics and pathogenic bacteria biosensing. SA@GO could effectively decrease time consuming for sweet spotting searching, reducing the amount of organic matrix and solvent and enhance the sensitivity. SA@GO shows high performance as a matrix alone without the needs to add trifluoroacetic acid (TFA). However, the analysis of the intact bacteria cells shows improvement in the signal intensity (2-5 folds) and offer low limit of detection. All these analyses could be performed with low concentrations (1-10 fmol) and tiny volumes (0,5–1 μL). This study demonstrated that the new exploration of new

hybrid materials is pivotal to achieve high performance and high ionization. Because the plane of GO, it assist protein-protein interactions that make it undergo softer ionization.

Keywords: graphene oxide, biosening, proteomics, biotechnology, pathogenic bacteria

Introduction

Due to the remarkable features such as high mass accuracy, high throughput analysis, fast analysis speed, and simplicity of operation; matrix assisted laser desorption/ionization mass spectrometry (MALDI-MS) has been extensively used in both laboratory and clinical analysis for the characterization of various analytes[1]. The matrix is defined as the material that can assist desorption/ionization process. It can be classified to 1) organic acids or 2) inorganic particles such as nanoparticles. Since their introduction as matrices, cinnamic acid derivatives, particularly 3,5-dimethoxy-4-hydroxycinnamic acid (sinapinic acid , SA) has been extensively used especially for proteins, oligodeoxyribonucleotides and peptide analysis [2]. However, searching for new MALDI matrices are still an active research field which can promote for highly progress of proteomics, medicine, biotechnology and other biomedical science [3]. Small organic acids are the most common matrices applied in MALDI-MS because of their advantages such as high sensitivity, convenience, and cost effectiveness. Techniques based on inorganic nanoparticles such as desorption/ionization on porous silicon (DIOS) or nanostructure-initiator mass spectrometry (NIMS) has been reviewed in Ref.[4]. This technique was coined as surface assisted laser desorption/ionization mass spectrometry (SALDI-MS). Since then a plethora of SALDI substrates has been reported in order to circumvent the challenges of conventional matrices. Moreover, the big challenges of conventional organic matrices such as SA are their solubility, and they are unstable in solution for long time as they may turn to crystals after few days.

Since it was synthesized in 2004 and awarded the Noble prize in 2010, graphene (G) and their derivatives graphene oxide (GO), are new allotropic members of carbon nanomaterials with a unique two-dimensional and one-atom-thick sheet structure, has been received giant attention from the scientific societies [5]. G and GO were utilized as MALDI matrices to detect low-mass molecules, such as amino acids, polyamines, peptides, steroids, nucleosides, nucleotides, metals and metallodrugs [6]. However, it can be only used for small molecules and it is also unstable for storage due to the irreversible stack of G nanosheets [7]. Due to the strong hydrophobic nature of G, G nanosheets have a strong tendency to aggregate to G clusters or even restack to graphite particles through van der Waals interactions. Thus, hydrophilic GO is more favourable that can be synthesized by modified the preparation method such as oxidation by acid i.e acid-oxidized graphene (AOG) [8]. The main advantages of G or GO is that it is able to be modified with other materials that can serve as both an absorbent in sample pretreatment and a matrix of MALDI-TOF-MS for the detection [9]. The various applications of G or GO were reviewed in Ref [10]. Recently, GO or rGO was reported for electrochemical detection of dopamine [11], single nucleotide polymorphism [12], discrimination of D- and L-cystine [13], Hg^{2+} sensors [14], NADH sensor [15], denosine detection [16], and combined with metal organic framework _(MOF) for Cu^{2+} sensor [17] and K^{+} [18].The combination among the same or different matrices provides multi-functionality, gain giant improvements of the analysis and circumvent some of these disadvantages [19]. It was reported that the conjugation between different matrices such as binary matrices by mixing common matrices with each other suppress the matrix peak interferences [20]. In addition, it forms homogenous spots, thus it does not need sophisticated sample preparation techniques [19]. Recently, Tseng et.al reported one pot synthesis of Au nanoclusters (Ag NCs) using conventional organic matrix (SA) [21]. They found that the Au NCs

in SA was capable of suppressing crystal growth, eliminating the coffee-ring effect, improve shot-to-shot reproducibility and enhancing the ionization efficiency of proteins [21]. Recently (2014), a multi-layer thin film of rGO and gold nanoparticles has been applied as the sample plate and matrixes in SALDI-TOF MS [22]. It has been applied for small molecules included raffinose, arginine, serine, valine, glucose, ribose, maltose and glutathione.

To the best of our knowledge, the possibility of utilizing GO to detect high molecular weight of proteins or pathogenic bacteria has never been tried before. Hence, in this work, we introduced a facile synthesis of highly dispersive sinapinic acid (SA) modified GO (SA@GO) solution that can be used for several months (>2 months) by hybridization the conventional matrix such as SA with GO (SA@GO). We aimed to find a facile approach to prevent the aggregation and crystallization of GO sheets and SA, respectively. The new hybrid material (SA@GO) is not only stabilize GO solution, but it is also prevent crystal growth, eliminating the hazard acids such as trifluoroacetic acid (TFA), improve shot-to-shot reproducibility and enhancing the ionization efficiency of proteins/pathogenic bacteria about 2-5 folds.

Experimental Section

Materials and methods

Sinapinic acid (SA), Trifluoroacetic acid, acetonitrile, lysozyme, α-lactalbumin, cellulase, trypsin were purchased from Sigma-Aldrich (USA). All chemicals were used directly without any purification. *Staphylococcus aureus* (BCRC 10451) and *Pseudomonas aeruginosa* (BCRC 10303) standard cultures were purchased from Bioresource Collection and Research Center (Hsin-Chu, Taiwan).

Instruments

The MALDI-TOF-MS analysis was performed by employing positive ion mode on a time-of-flight mass spectrometer (Microflex, Bruker Daltonics, Bremen, Germany) with a 1.25 m flight tube. Desorption/ionization was obtained by using a 337 nm nitrogen laser with a 3 ns pulse width. The accelerating potential is +20 kV. Laser power was adjusted to slightly 10% above the threshold to obtain good resolution and signal-to-noise ratios. The data were repeated more than three times to confirm repeatability. Data were collected using Microflex-Control software (Bruker Daltonics, Bremen, Germany) and processed with Flex Analysis software (Bruker Daltonics, Bremen, Germany). Data were drawn using Origin V 6.0 program.

The pH of the solutions was measured by a pH meter (720P, Istek, South Korea). The UV measurements were undertaken in an UV spectrophotometer (Perkin Elmer 100, German). The Fourier transform infrared (FT-IR) spectra were recorded on a FT-IR spectrometer (Spectrum 100, Perkin Elmer, USA). The scanning electron microscope (SEM) images were acquired using a SEM (JOEL 6700F, Japan). The size and the morphology of nanoparticles were determined by transmission electron microscope (TEM, Philip CM200, Switherland). XRD has measured by Bruker AXS D8 Advance, German.

Protein and enzyme preparation

Different protein and enzymes such as lysozyme, α-lactalbumin, cellulase, and trypsin were analysis. The stock solution of the analyte was prepared in deionized water by concentration 1×10^{-3} M.

Bacteria culture

Staphylococcus aureus (BCRC 10451) and *Pseudomonas aeruginosa* (BCRC 10303) standard cultures were purchased from Bioresource Collection and Research Center (Hsin-Chu, Taiwan) and were cultivated at 37°C and maintained on DifcoTM Nutrient broth (Becton and Dickinson,

France, 8.0g per 1.0L) and Agar plates (Gen Chain Scientific (GCS), New York, USA, with 1.5% agar). Both bacteria cells were grown individually overnight at 37 °C using agar medium and then the bacteria cells were collected by via noodle then re-dispersed in sterile and deionized water (1 mL).

Preparation of conventional matrices sinapinic acid (SA)

Sinapinic acid was prepared according to the conventional procedure [2]. Briefly, 50 mM concentration was prepared by dissolve 120.5 mg mL^{-1} in aqueous acetonitrile (10 mL, 50:50) with 1% TFA. The solutions were stored in the refrigerator for usage (maximum two weeks).

Preparation of SA@GO

The oxidation of natural graphite to graphene oxide was performed from the modified method of Hummers;[23] the method was based on strong oxidation of graphite by $KMnO_4$ in strong acid,. The reduced graphene (0.1 g) has been suspended in 10 mL of deionized water then sinapinic acid (0.12 g) were added and the solution was stirred (24 h) till SA dispersed in the GO solution as shown in Fig. 1A.

Bacteria cell detection

The solutions of different bacteria were detected individually. About 0.5 µL of *P. aeruginosa* (1×10^4 cfu/mL) and *S. aureus* (1×10^5 cfu/mL) was mixed with 0.5 µL SA and SA@GO. The mixture was spotted in stander stainless steel plate and leaved for dry before the analysis (See Fig.1B).

Protein and enzyme detection

From the stock solution, 0.5 µL of the analyte solution (lysozyme, α-lactalbumin, cellulase, and trypsin) was mixed with 1 µL of SA or SA@GO. The mixture was spotted in standard MALDI plate. The spot was leaved for dry before the MALDI measurement (See Fig.1B).

Results and discussion

Characterization of SA@GO nanocomposites

The synthetic strategy for the preparation of the SA@GO nanocomposites is presented in Fig. 1A. The SA@GO material was synthesized using simple stirring of GO solution and solid SA, and then characterized by different techniques, including electron microscopy (EDX, SEM and TEM), and X-ray diffraction (XRD). It is very simple methods for the synthesis of highly dispersive GO which can be stable for more than two months (Fig. 1A). We aimed to find a facile approach to prevent the aggregation of GO sheets while maintaining the GO structure and in the same time prevent the crystallization of SA and make it soluble in water instead of using organic solvent. Furthermore, an acid such as TFA that was frequently used to enhance the homogenous of the analyte-matrix was not required in the current approach. We found that the SA@GO aqueous dispersion was rather stable even after storing at room temperature for two months, no crystallization of the conventional matrix i.e SA which indicated that the intercalation between the layers and the electrostatic repulsion between the polar groups in SA@GO sheets is strong enough to prevent the aggregation of SA@GO sheets.

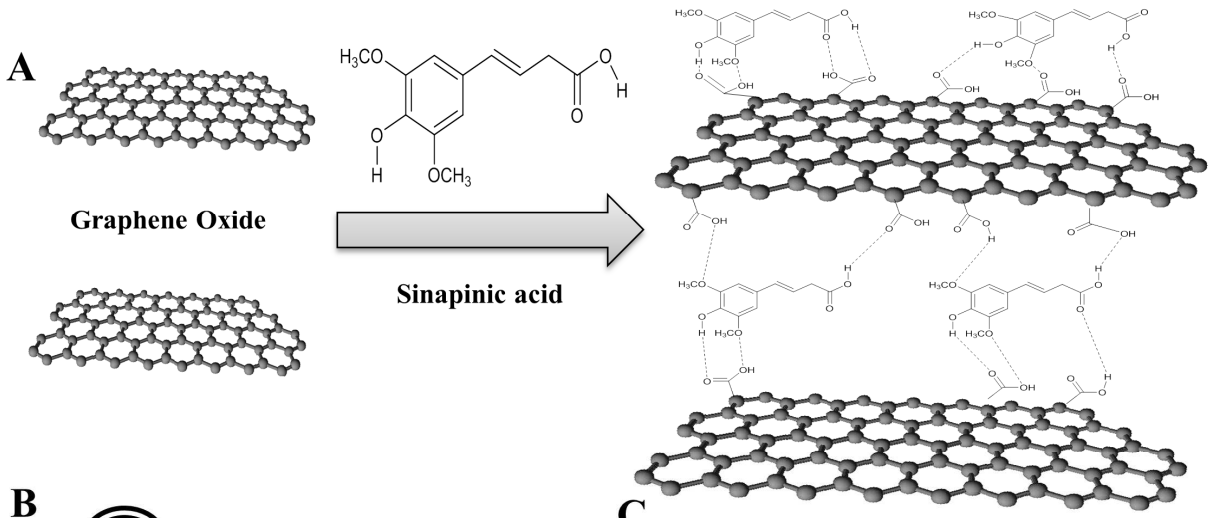
A
Graphene Oxide
Sinapinic acid

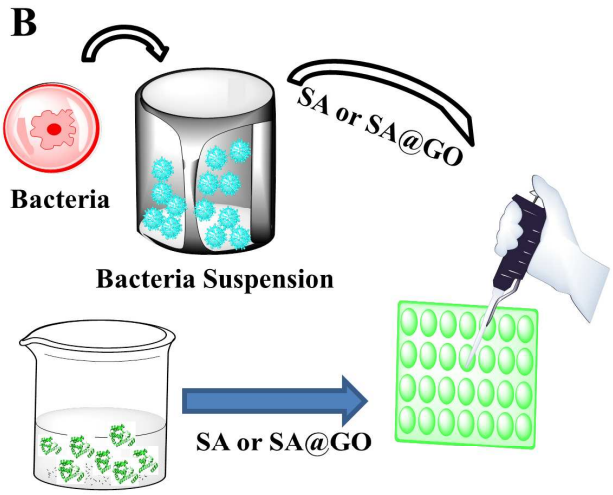
B
Bacteria
SA or SA@GO
Bacteria Suspension
SA or SA@GO

C

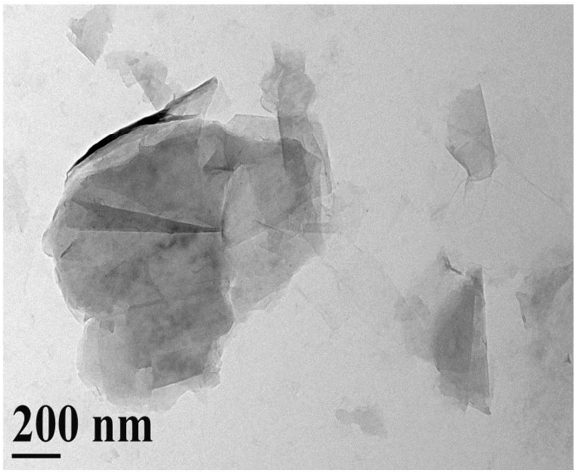
200 nm

D

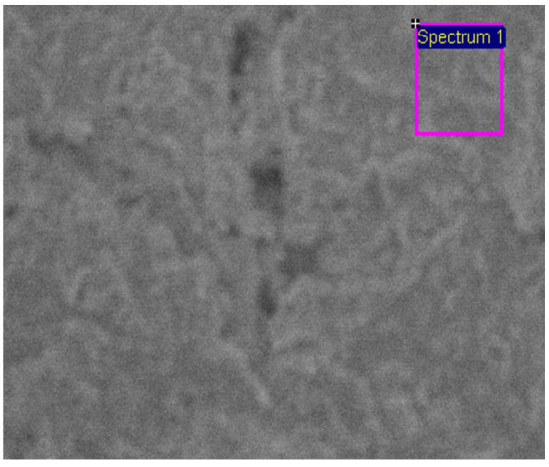
Spectrum 1

E

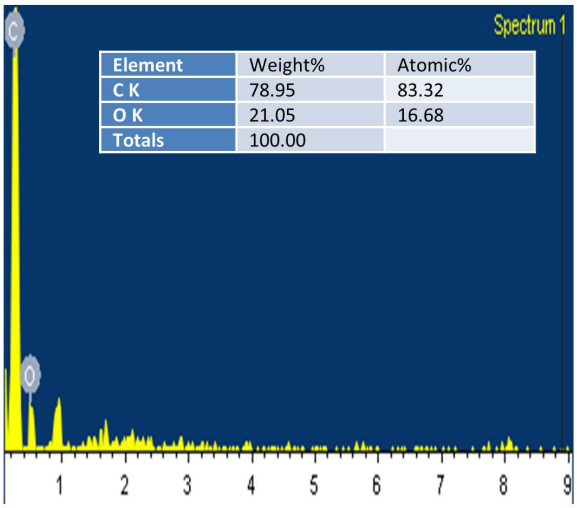
Spectrum 1
Element | Weight% | Atomic%
C K | 78.95 | 83.32
O K | 21.05 | 16.68
Totals | 100.00
1 2 3 4 5 6 7 8 9

F

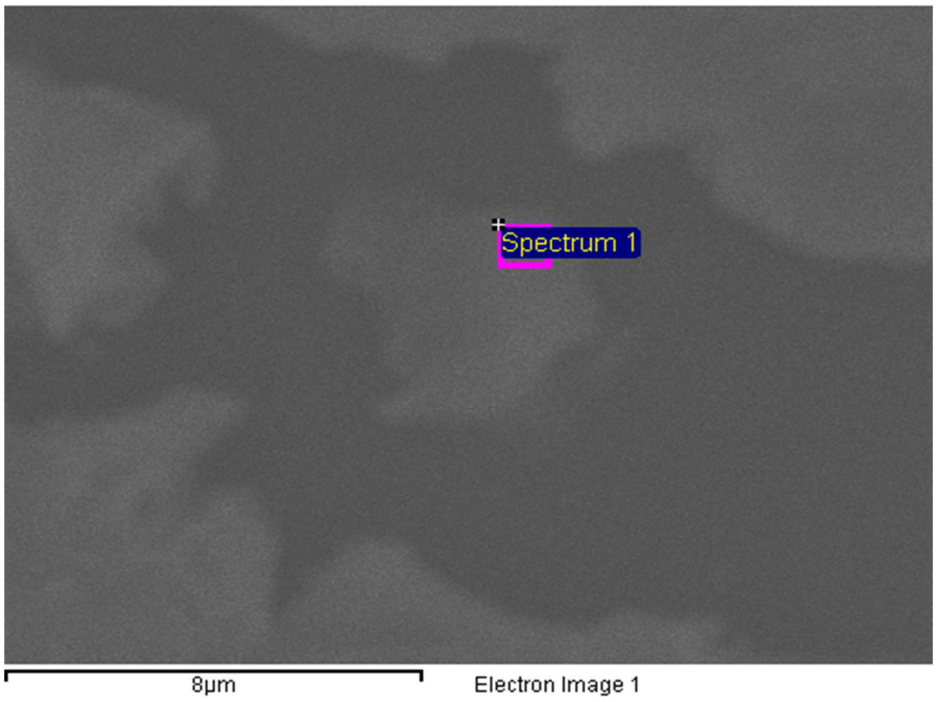
Spectrum 1
8µm
Electron Image 1

G

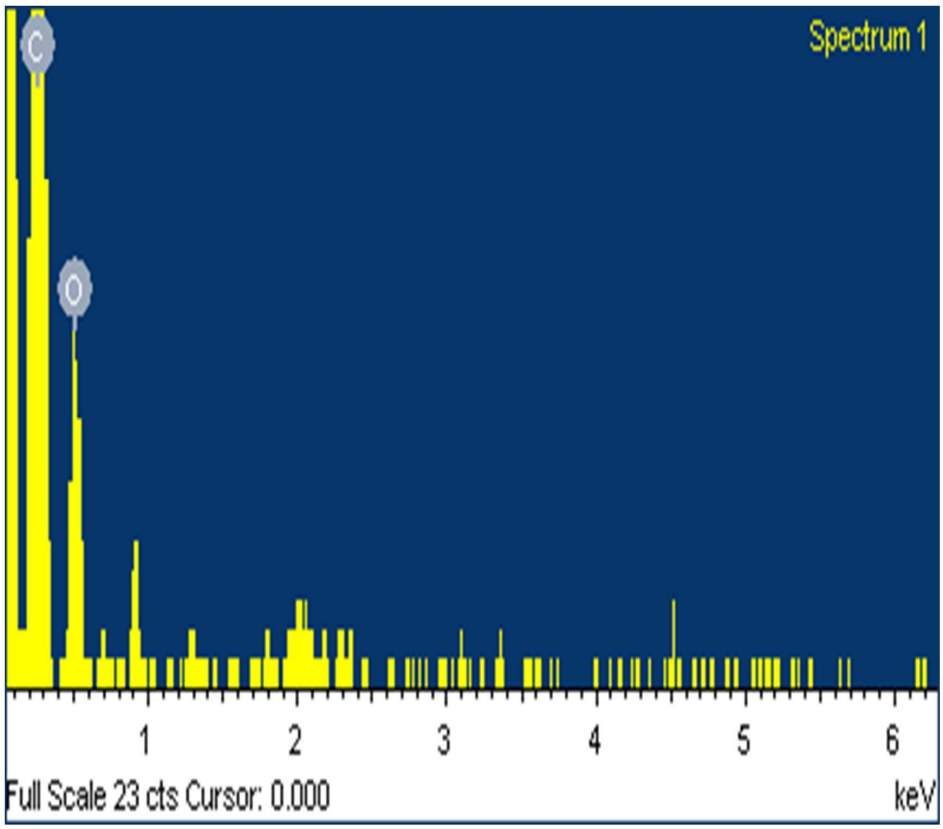
Spectrum 1
C
O
1
2
3
4
5
6
Full Scale 23 cts Cursor: 0.000
keV

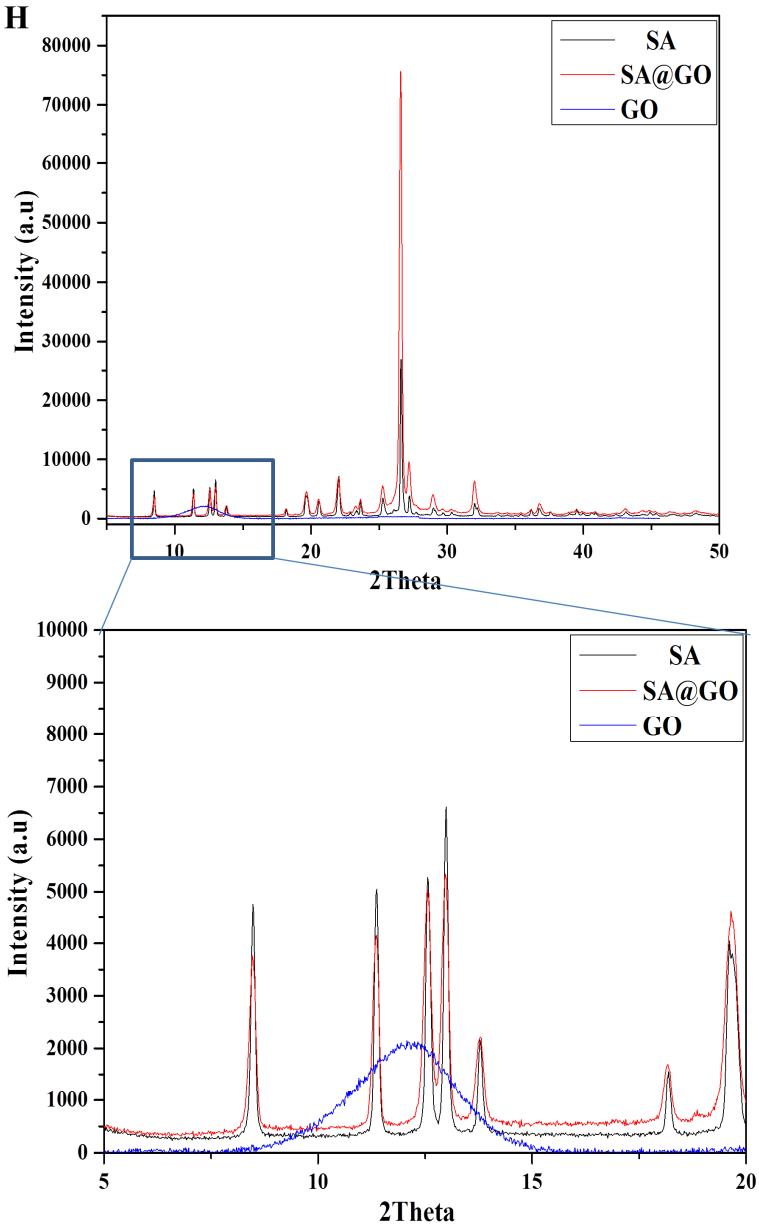

Figure 1 (A) Schematic representation of SA@GO synthesis, (B) Schematic representation of protein, enzyme and bacteria detection using SALDI-MS, the pathogenic bacteria were cultivate and collected by noodle then dispersed in deionized and sterizled water then 0.5µL mixed of the suspension or the protein mixed with or with 0.5µL of GO or SA@GO and are spotted in

standard MALDI plate, (C) TEM image of SA@GO, SEM and EDX analysis of GO (D, E) and SA@GO (F, G), and (G) XRD analysis of the synthesized material.

The size and morphology of the as-prepared SA@GO was investigated by TEM (Fig. 1C). The obtained composite retained the two-dimensional sheet structure with micrometers-long wrinkles. The chemical analysis and the morphology of the synthesized materials were characterized before (Fig.1D, Fig.1E) and after the modification (Fig.1F, Fig.1G) by using SEM and EDX. The data clearly indicate that a tiny amount of oxygen was present in pure GO (16%), while the amount of oxygen was enhanced after modification in SA@GO. The purity of GO, SA and SA@GO were reported using XRD (Fig.1H). The XRD measurement of GO (Fig. 1H) revealed a strong and broad diffraction peak at around 12 degrees, which indicate of a few number of oxidized graphitic layers. Sinapinic acid, or chemically 3,5-dimethoxy-4-hydroxycinnamic acid, is infinite one-dimensional chains of two types of dimeric eight membered O–H/O hydrogen bonding rings between the neighboring carboxylic groups as well as the hydroxyl and solvent methanol oxygen atoms, respectively, but it showed no π-stacking in its layer packing . It is believed that van der Waals forces contribute to this kind of layer packing. Thus, it is easy to stack on the surface of GO nanosheet. The peak intensity of XRD (Fig.1H) are changed. The absence of GO peaks may be due to the low concentration of GO or peak submerge. The materials were characterized using FTIR as shown in Fig.2A. The distinct change in the FTIR preliminarily confirms the successful stack of SA on the exterior surface of GO. Pure SA shows peaks at 3400, 3000, 1750, 14500, and 1200 cm^{-1} that were assigned as O—H, C—H, C=O, C=C, and C—O, respectively (Fig.2A). Most of these vibrational peaks were vanished after SA stack on the surface of GO that implies the π-π interactions. UV-vis absorption

of GO and SA@GO (Fig.2B) were reported. SA displays absorption at 337 nm that matched with the N_2 laser that use for MALDI-MS, thus it was served as a matrix [2]. GO displays a continuous absorption with a maximum peak at 220 and 270 nm that assigned as n-π* and π- π* transition, respectively (Fig. 2B). GO shows also continuous absorption, it is IR absorber. However, it can be serve as a matrix for low molecular weight because the large surface area can assist desorption/ionization process [6]. SA@GO displays a different absorption as it still shows the maximum peak at 337 nm and it continuous absorbs in the visible range (Fig.2B). To demonstrate the potential advantage of this material, we herein show the application of SA@GO as a matrix in MALDI MS for proteomics, enzymes and pathogenic bacteria analysis.

Application of SA@GO for proteomics and enzymes analysis

Schematic representation of SA@GO application for protein and pathogenic bacteria was presented in Fig.1B. In order to investigate the applicability of SA@GO as a novel substrate for MALDI-MS, various biomolecules such as cellulose (40000Da, Fig.3A), trypsin (23000Da, Fig.3B), α-lactalbumin (14000Da, Fig.4A) and lysozyme (14000Da, Fig.4B) were investigated and the results are listed in Table 1. Cellulase is an enzyme that is produced s mainly by fungi, bacteria, and protozoans that catalyze cellulolysis (break down the cellulose molecule into monosaccharides). This process is utilized in sustainable industries based on lignocellulosic feedstock. Thus, high performance in analysis is necessary to understand basic cellulase mechanisms, and deliver rational improvements of the industrial process [24]. Modified graphene has been reported recently as a new electrochemical approach to the quantification of the populations of the free cellulose enzyme that are present in the aqueous bulk [24]. They reported an affinity between cellulase and graphene, thus they are able to distinction of the three states appears that are essential to the identification of the rate-limiting step. Graphene oxide assisted

laser desorption/ionization mass spectrometry (GALDI-MS), that is based on the use of SA@GO as matrix, shows a peak at 40000Da corresponding to $[cellulose+H]^+$ (Fig.3A). The spectra indicated a high intensity (2 folds) higher than conventional organic matrix SA. It is also noted that it has good resolution (Fig.3A).

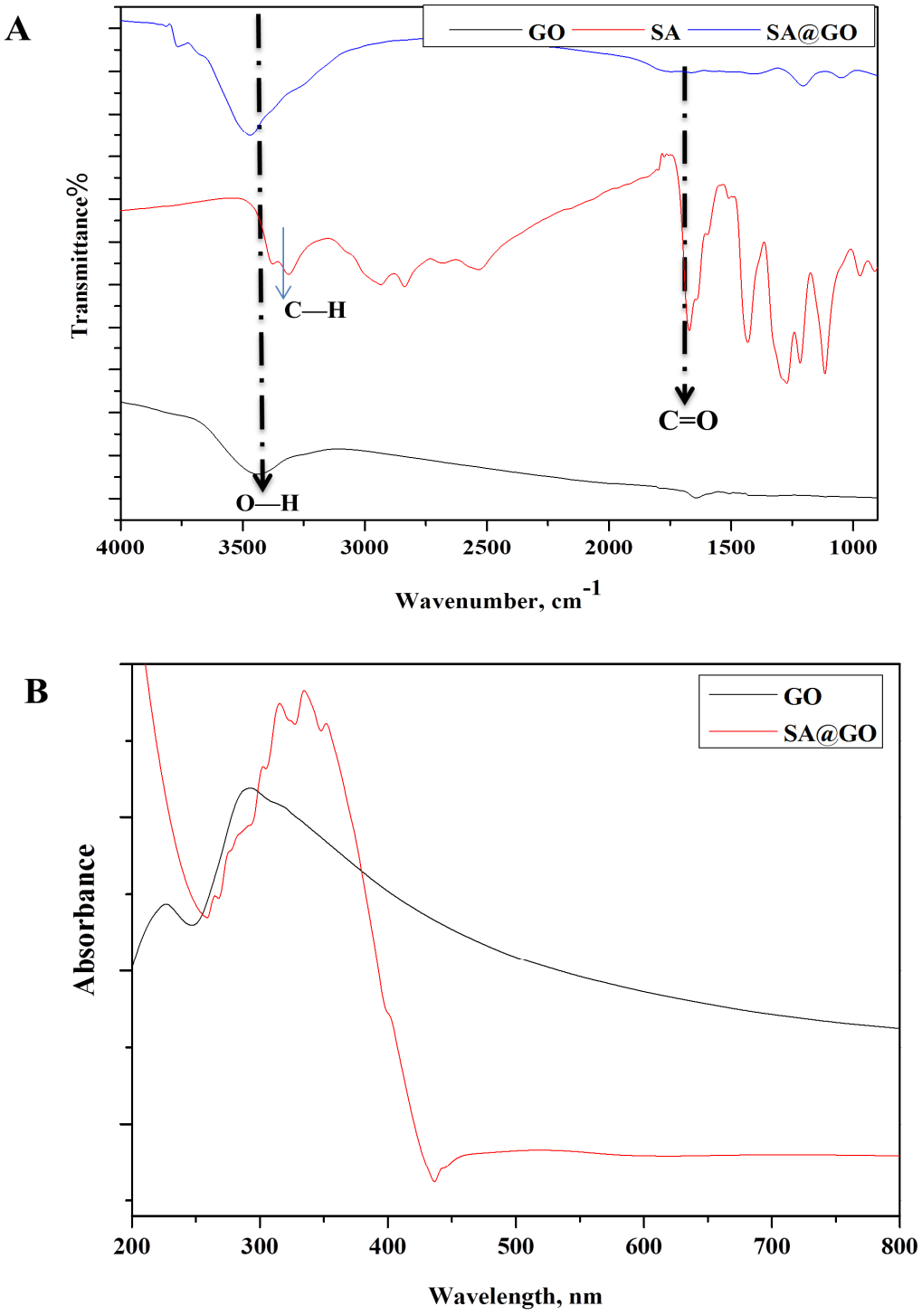

Figure 2. (A) FTIR spectra and (B) UV-vis absorption of GO, SA and SA@GO.

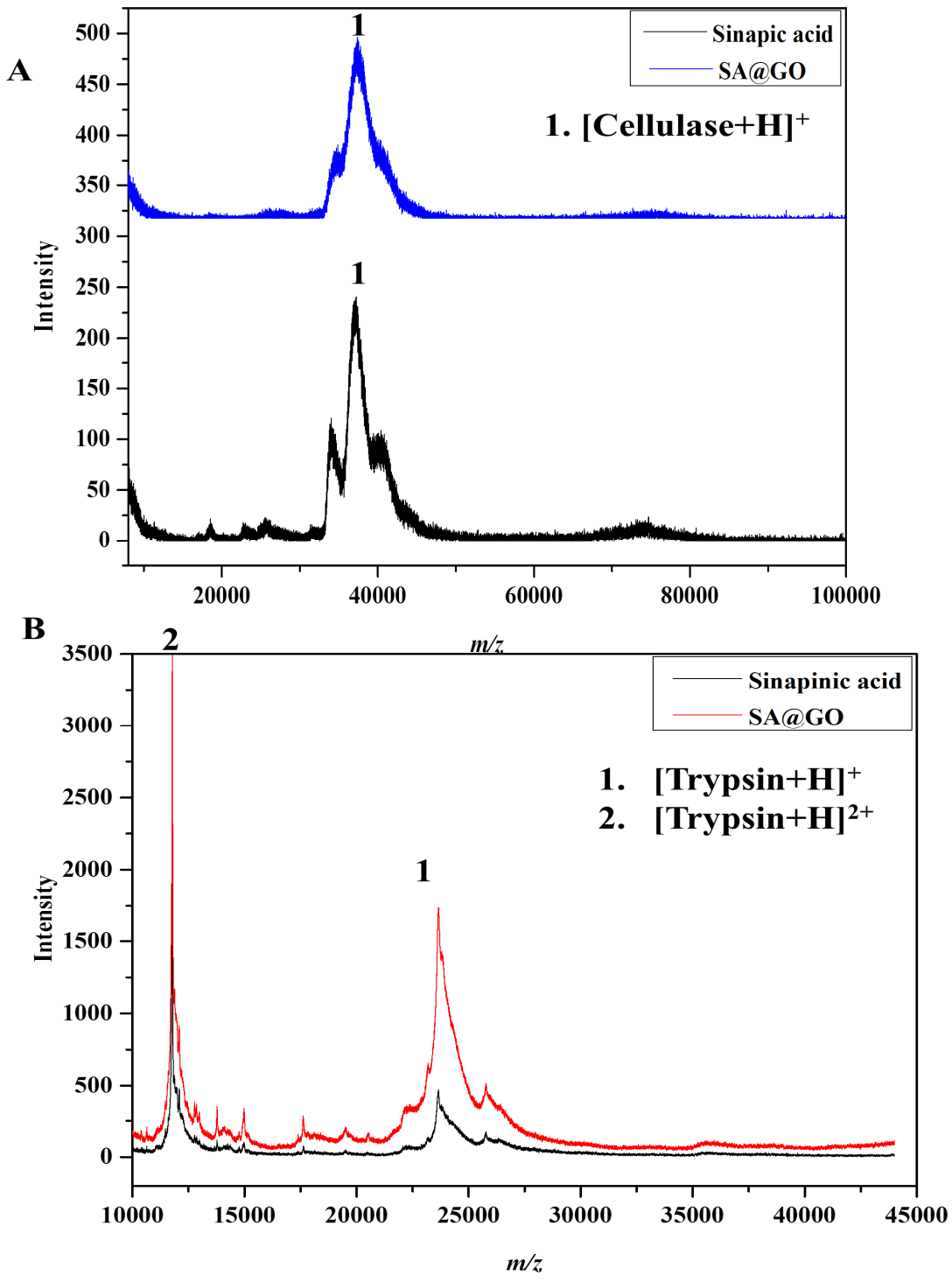

Figure 3. MALDI analysis of (A) cellulase and (B) trypsin using SA and SA@GO, condition: [C] = 1×10^{-4}M, V=0.5μL

Trypsin is proteases enzyme, known as proteinases or proteolytic enzymes that play critical roles in many physiological processes such as cell growth and differentiation, cell–cell communication, and cell death [25]. Zhang et.al [25] reported a label-free streptavidin-modified magnetic beads (Str-MBs)-based sensing platform for turn-on chemiluminescent (CL) detection of trypsin with limit of detection 10 pM in 30 mins. GALDI-MS spectra of trypsin solution (Fig.3B) shows two peaks at 11500 and 23000 Da corresponding to $[trypsin+H]^{2+}$ and $[trypsin+H]^{+}$, respectively. In contrast to fluorescence technique, GALDI-MS can use a tiny amount of the sample (0.5 μL) with limit of detection 5 fmole that indicate high sensitivity of MALDI over than fluorescence technique (Table 1). Furthermore, it is high throughput analysis over than fluorescence that can only run one sample per run.

α-lactalbumin is casein protein that can exist in mammalian cells and was recognized as the most common cow milk allergens. Yang et.al [26] reported a new approach called fluorescence-linked immunosorbent assay (FLISA) for the detection of α-lactalbumin was established reported high-affinity monoclonal antibody (mAbs) conjugated with quantum dots (QDs) against α-lactalbumin that linked by using N-(3-dimethylaminopropyl)-N-ethylcarbodiimide hydrochloride (EDC) as an activator and N-hydroxysuccinimide (NHS) as a coupling reagent. GALDI-MS spectrum of α-lactalbumin (Fig.4A) show peaks at 7000, 14000 and 28000Da that were assigned as $[\alpha\text{-lactalbumin}+H]^{2+}$, $[\alpha\text{-lactalbumin}+H]^{+}$, $[\alpha\text{-lactalbumin-}\alpha\text{-lactalbumin}+H]^{+}$, respectively. Because the conformational plasticity of α-lactalbumin, bovine α-lactalbumin (BLA) could interact with the cellular proteins [27]. These interactions (BLA–membrane interaction) would help in bioengineering of α-lactalbumin, and to address the mechanism of tumoricidal and antimicrobial activities of BLA–oleic acid complex[27]. The covalent complexation between (-)-epigallocatechin gallate (EGCG) and α-lactalbumin were also reported at 24 h, pH 8.0 and 60 °C [27].

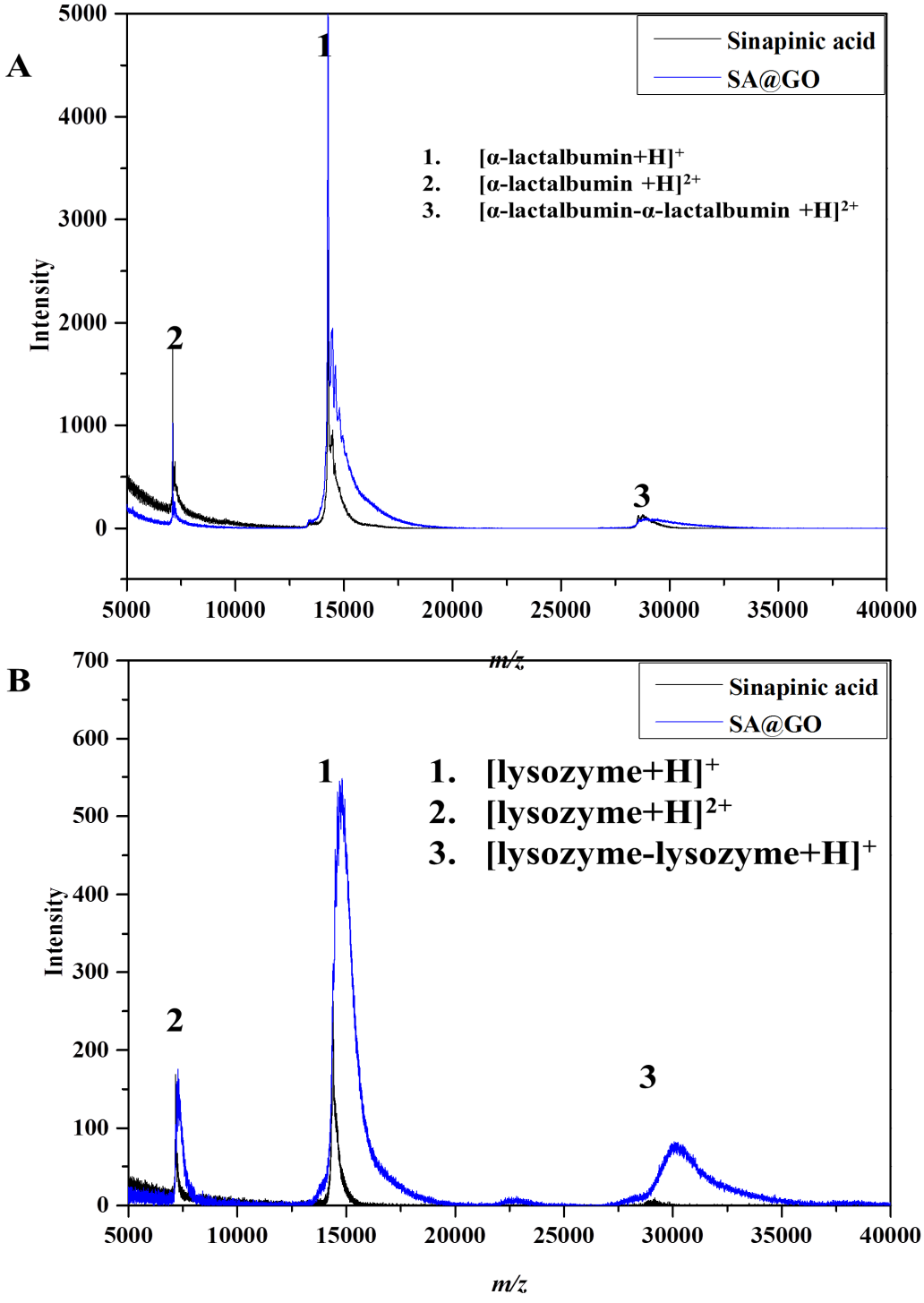

Figure 4 MALDI analysis of (A) α-lactoalbumin and (B) lysozyme using SA and SA@GO, Condition: [C] = 1×10^{-4} M, V=0.5μL

Here, we can note the great affinity of the protein to undergoes to homodimer proteins (protein-protein) interactions i.e [α-lactalbumin- α-lactalbumin +H]$^{+}$. SA@GO displays high sensitivity over the reported method (Table 1).

Lysozyme (also called 1,4-β-N-acetylmuramidase, 14000 Da), an ubiquitous protein in mammals and is often termed body's own antibiotic, is a relatively small single chain protein with only 129 amino acids. It is an important defense molecule of the innate immune system and the lysozyme level in serum and urine could be used as potential indicators for leukemia, renal disease, sarcoidosis and meningitis [28]. Thus, the reliable and sensitive methods for the analysis of lysozyme are necessary. Li et.al [29] reported a facile approach for fluorescent sensing of lysozyme using CdTe QDs and lysozyme binding DNA (LBD) as a probe. The probe was synthesized by via the negatively charged of LBD that could conjugate with the positively charged CA–capped CdTe QDs. In the presence of lysozyme, the QDs–LBD complex could bind specifically with lysozyme to form ternary complex of QDs–LBD–lysozyme, and thus the fluorescence intensity was enhanced. Another ultrasensitive "turn on–off" fluorescence nanosensor was reported [30]. The novel nanosensor was constructed with the carboxymethyl chitosan modified CdTe quantum dots (CMCS-QDs). However, these methods are sensitive, simple, and selective. But it is expensive, time consuming, pH and temperature sensitive and lack robustness. Recently, a study revealed that GO demonstrated a strong interaction with lysozyme [31]. This interaction is so strong thus it can selectively eliminate and separate lysozyme from aqueous solution onto the surface of GO from a mixture of binary and ternary proteins. The primary forces are electrostatic interactions. GALDI-MS spectrum (Fig.4B) of lysozyme shows peaks at 7000, 14700 and 29400Da that assign as [lysozyme+H]$^{2+}$, [lysozyme+H]$^{+}$, and [lysozyme-lysozyme+H]$^{+}$, respectively. It is noted that the acidity of SA destroy the non-covalent interaction, thus the last

peak is absent. Zenobi group [32] reported the non-covalent interactions of lysozyme and lysozyme binding aptamer (LBA) using nonacidic matrix 6-azathiothymine (ATT) that was able to preserve the non-covalent interactions. The data reveal that GO in SA@GO mediate the acidity of conventional organic matrix i.e SA and can serve as a mat that can assist the detection of protein-protein interactions. The spectra reveal 4 folds increase of their sensitivity over than SA (Fig.4B) and other reported method (Table 1). Recently (2014) Lee et.al reported that the folded conformation of Lyz was maintained in pH 2.2 while formic acid and acetic acid, which are weak acids ($pKa > 3.5$), induce unfolding of Lyz during electrospray ionization ESI [33]. They also reported that strong acids such as HCl suppressed formation of the unfolded conformers because HCl is the high dissociation of HCl in solution, furthermore Cl^- within the ESI droplet can interact with Lyz to reduce the intramolecular electrostatic repulsion [33]. Because the adosprion of Lyz in the surface of GO, Lyz-Lyz is detectable. Thanks to this adosprion, thrombin could be detect by electrochemical methods [34].

Pathogenic bacteria analysis

Analysis of pathogenic bacteria using MALDI-MS is fast, required only a few microliters approximately 10–20 times cheaper than the analysis by the conventional methods identify the bacterial cells based on their biomarker peaks or protein profiles [35]. It can provide three types of characterization: (1) strain categorization, (2) strain differentiation, and (3) strain identification [35]. This feature is general not only for bacterial cell, but also for other cells such as human hepatocyte carcinoma cell line (HepaRG) [36]. These proteins can be used as a "proteomics fingerprint" that can be used to characterize the investigated cells [36]. The biomolecules of the intact cells are lysed physically (e.g, sonication, agitation, vortexing, or other physical methods)

or chemically (e.g, via exposure to organic matrices, or TFA or formic acid/organic solvents that are used during the matrix preparation). These processes release partially the contents of the cells into the supernatant, thus it can be detected during MALDI-MS analysis. Pathogenic bacteria analysis of *S. aureus* (Fig.5A) and *P. aeruginosa* (Fig.5B) were investigated. The spectra reveal the improvement for the MALDI-MS signals for 2 and 5 folds for *S. aureus* (Fig.5A) and *P. aeruginosa* (Fig.5B), respectively. Note that using the SA@GO matrix, no need to add the TFA acids, while we can still obtain successful peaks related to cell membranes. It is important to stress that there are two methodologies for the bacteria biosening: 1) analysis the intact cell, or 2) targeting a specific biomolecules such as protein, or DNA [37]. The latter strategy is mainly use for other techniques, while the former is predominant in mass spectrometry such as MALDI-MS. Herein; we use MALDI-MS to detect the whole cell or precisely intact cell. Because the huge number of the cell biomolecules, ion suppression could be take place. Thus, few number of the cell protein were detected. In traditional matrix such as SA, trifluoroacetic acid assist cell hydrolyzes. However, it has environmental and human health concerns. In contrast, SA@GO requires no TFA and showed the same peak pattern with high intensity (2-5 fold).

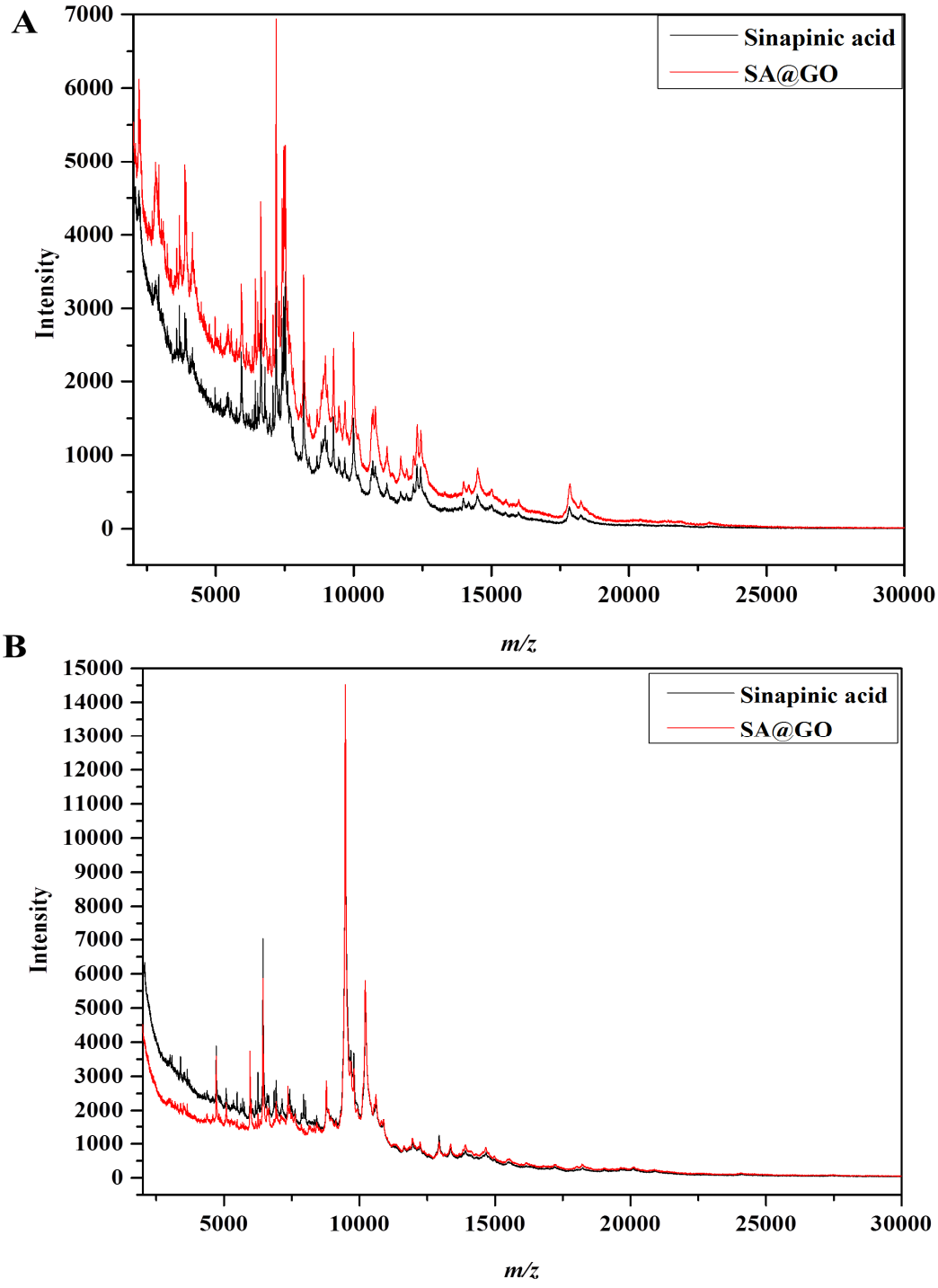

Figure 5. MALDI analysis of (A) *S.aureus* (1×10^5 cfu/mL) and (B) *P.aeruginosa* (1×10^4 cfu/mL) using SA and SA@GO using 0.5 μL for spotting.

In order to gain more clear view of the interactions among the pathogenic bacteria and the new composition SA@GO, transmission electron microscopy (TEM) of the bacterial cells and their interactions with GO and SA@GO were reported (Fig.6). GO and SA@GO could interact the bacteria cells mainly by the hydrophobic interactions. It could also interact via an electrostatic interaction among the negative charges of the bacteria and the positive charges on the GO surface. It is important to note that the surface of the bacteria cells hold a net negative charges due to ionized phosphoryl and carboxylate substituent on the outer cell envelope macromolecules or due to techoic acid of Gram positive and lipopolysaccharide in Gram negative. TEM analysis (Figure 6) of the bacteria cells (A) *P. aeruginosa*, and (B) *S. aureus* before (a) and after the interaction with (b) GO and (c) SA@GO were reported. TEM images show the high affinity of the different bacteria to GO and SA@GO that immobilized on the cell membrane. The images reveal also low toxicity of SA@GO over than GO. It is also indicate the high absorption of the G-based material for the biological biomoleculs, thus it could improve the desorption/ionization process and require no crystallization with the conventional matrix. Recently (2014), Tu et.al reported different modification of GO with chemical modification with amino- ($–NH_2$), poly-*m*-aminobenzene sulfonic acid- ($–NH_2/–SO_3H$), or methoxyl- ($–OCH_3$) terminated functional groups [38]. They found that positively charged GO was found to be more beneficial for neurite outgrowth and branching [38].

Pros and cons

The ideal MALDI-MS matrices are the materials that have strong energy absorption and transfer capability. In this regard, SA is a good example due to its absorption that matches the wavelength of N_2 laser, thus it have been used intensively for protein and high molecular weight compound analysis. However, SA offer some drawbacks such as lack of solubility, tend to

crystallize during short storage time and their acidity destroy the non-covalent interaction among the different molecules. In a stark contrast, GO did not display absorption that matched very well with N_2 laser, but it could work for small molecular weight due to the large surface area, fast charge carrier mobility and universal and frequency-independent optical absorption properties. Furthermore, GO has efficient electron-phonon coupling and high thermal conductivity. However, GO can cause less fragmentation of thermal labile molecules and can produce low background interference in the low-mass region. By conjugate SA and GO in the new material that was coined as SA@GO, all or some of these drawbacks have been solved.

The dispersion of the conventional matrix SA is improved by loading on the interior plane of GO. The main forces that assist this combination are π-π and electrostatic interactions. The reason for this is attributed to the better dispersion of the SA@GO matrix relative to the GO and SA matrices, causing higher laser energy absorption and transfer efficiency. Liu et.al reported the dispersion of magnetic nanoparticles on the GO surface and their application for screening enzyme inhibitors [39]. They claimed that the effective desorption/ionization of analytes was mainly attributed to the π-conjugated networks of magnetic graphene matrix, which could absorb the energy from UV laser radiation and transfer it to the analytes to assist the process of desorption/ionization. Our group also reported the dispersion of insoluble nanoparticle SnO_2 by using GO as the surface [39]. The data reveals high resolution of the pathogenic bacterial over than the spectra that was obtained from only the conventional matrix SA [39]. Combination of the conventional matrix SA with GO in the new material SA@GO could also reduce the direct interaction of SA and the target analyte. Fagerquist et.al [40] reported the apparent formation of matrix adducts of 3,5-dimethoxy-4-hydroxycinnamic acid (sinapinic acid or SA) and α-cyano-4-hydroxycinnamic acid (CHCA) matrix via covalent attachment to disulfide bond-containing

proteins (HdeA, Hde, and YbgS) from bacterial cell lysates ionized by MALDI-MS, time-of-flight-time-of-flight tandem mass spectrometry (TOF-TOF MS/MS) and postsource decay (PSD).

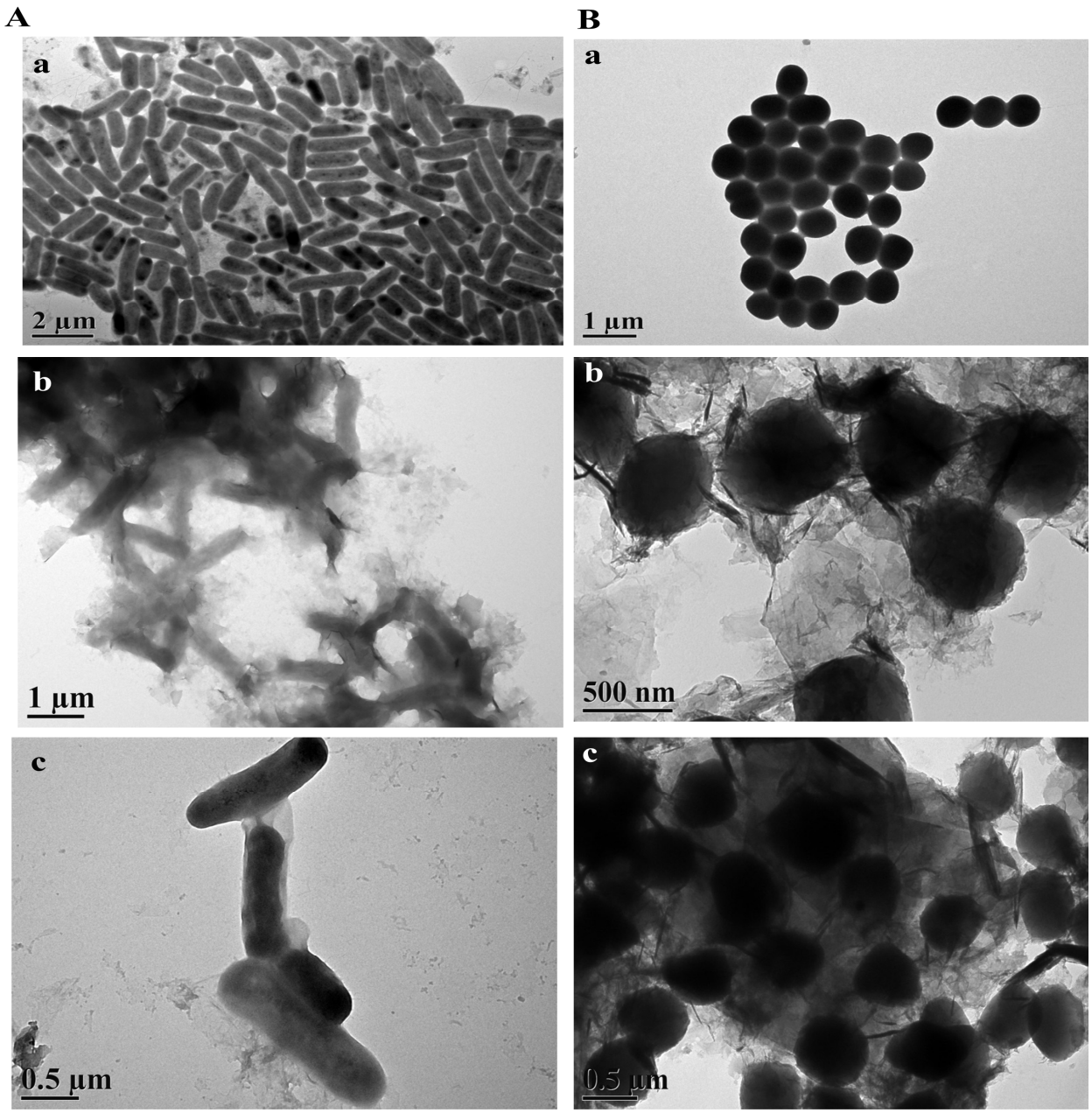

Figure 6. TEM analysis of (A) *P. aeruginosa* and (B) *S. aureus* before (a) and after the interaction with (b) GO and (c) SA@GO

The observation on the absence of adduct formation when using CHCA and they explained that due to the electron withdrawing effect of the α-cyano group of this matrix that may inhibit salt formation and/or amide bond formation. In contrast, they found these interactions in the other matrix i.e SA that has no cyano. By using further mass spectrometric analysis of disulfide-intact and disulfide-reduced over-expressed HdeA and HdeB proteins from lysates of gene-inserted *E. coli* plasmids, they found that the covalent attachment of SA occurs not at cysteine residues but at lysine residues [40]. Stack SA on the surface of GO in SA@GO could also do the same effect of cyano group as the π resonance of SA will consume long time due to conjugation with the π resonance of GO. It is also important to note that GO sheet may be use as a mat that can assist the biomolecules to interact together and make it stable for further detection of protein-protein interactions.

The large surface area of SA@GO improves the spectra reproducibility of the conventional matrix SA. Toh-Boyo et.al [41] investigated the reproducibility of mass spectral profiles of the whole bacterium *E. coli* resulting from laser sampling at different regions with different deposition methods and using different MALDI matrices [41]. The three most common matrices used in MALDI- MS bacteria profiling, CHCA, SA, and ferulic acid (FA), were compared along with two pipet-based sample deposition methods (dried-droplet and premix) and spray nebulizer sample deposition method. For the two pipet-based sample deposition methods tested, the intrasample variability ("spot-to-spot" reproducibility) was of the same magnitude as the intersample variability for all MALDI matrices tested. In contrast, a spray nebulizer sample deposition method produces uniform sample/matrix mixtures onto the MALDI plate, thus it improves the intrasample reproducibility. The most interested observation is that SA matrix yielded the largest variations in mass spectral profiles regardless of the pipet-based methods

used, when compared to the other MALDI matrices tested. These variations are completely not observed here. The prime reason may be due to the large surface are of SA@GO. It is also reported for SA modified Au nanocrystals [21]. Probably, it is due to the same reason.

The material SA@GO require no acidic additive, thus it is softer over than acidic matrix SA. It is difficult to draw a relationship between the pH or acidity and the mass signal or discrimination. This is because the mass detection is function on many other parameters such as sample preparation, target properties, molecular weight, matrix type, laser wavelength and so on. It is well known that highly acidic matrix solutions (pH <1.8) showed weak or no signal for peptides <2 kDa and mainly favored the appearance of components with masses >2 kDa. However, matrix solutions that contained formic acid and had pH <1.8 consistently yielded the strongest response to high-mass components [42]. It was noted that matrix solutions with pH between 1.8 and 2.3 exhibited mass spectrometric peaks is the optimal condition for the low- and intermediate mass over the high-mass components. The matrix solutions with pH >2.3 is strongly favored for the appearance of peptides below 2 kDa. Three MALDI-MS sample/matrix preparation approaches were evaluated for their ability to enhance hydrophobic protein detection from complex mixtures: (1) formic acid based formulations, (2) perfluorooctanoic acid (PFOA) surfactant addition, and (3) sorbitol addition [43]. They found that sorbitol (1.5% w/v sorbitol) in the SA solution promote homogeneous crystallization and to enhance medium and higher *m*/*z* ion detection from dilute *E. coli* cellular mixtures. The signal-to-noise (S/N) ratios in SA dropped to approximately 20:1 using 1% and 5% TFA, respectively. However, it is completely different in the cases for bacteria analysis [44]. Acidification of the solvent is assumed to assist in extraction of proteins from the cell wall and to increase the efficiency of ionization. Thus, increasing the

concentration of TFA to 2% from the routinely used 0.1% provided more informative spectra than did application of cell lysis methods.

Because the homogenous formation of hybrid matrix, no need to use sophisticated instruments such as nebulizer. Li et.al [45] reported the application of the hybrid matrix to biological samples using silicon dioxide and 9-aminoacridine. They claimed that it possesses less threat to the experimenters and the environment since the toxic matrix compounds does not need to be sprayed by using a gas-powered sprayer, which could lead to the contamination of the laboratory environment with toxic aerosols [45]. Because the noncovalent interaction of different biomolecules with GO, it can assist the biomolecules-biomolecules interaction as reported for Lyz [46]. These interactions or adsorption, GO can be used for enzymatic and nonenzymatic detection of important biomolecules such as DNA [47].

Conclusion

As one of the most amazing material, graphene oxide has revealed new and exciting features. The sinapinic acid modified graphene oxide (SA@GO) exhibited mass spectrometric peaks that spanned the greatest latitude in mass range, although tending to favor the intermediate and high mass components. We can expect further applications of this matrix, particularly in biotechnology of pathogenic bacteria analysis with MALDI-TOF-MS. The GO nanosheets are able to serve as a two-dimensional “mat” with which the SA interacts to hinder the aggregation. SA@GO can significantly improve the sensitivity and enhances their performance in MALDI-MS.

Acknowledgments

The authors are particularly grateful to the Ministry of Science and Technology of Taiwan for financial support.

References:-

1. Norris, N.L.; Caprioli, R.M. Chemical Reviews 2013, **113**, 2309–2342
2. (a) Salum, M.L.; Itovich, L.M.; Erra-Balsells, E. J. Mass Spectrom. 2013, **48**, 1160–1169; (b) Beavis, R.C.; Chait, B.T. Rapid Commun. Mass Spectrom. 1989, **3**, 432; (c) Beavis, R.C.; Chaudhary, T.; Chait, B.T. Org. Mass Spectrom. 1992, **27**, 156; (d) Schneider, K.; Chait, B.T. Rapid Commun. Mass Spectrom. 1993, **28**, 1353.
3. (a) Abdelhamid, H.N.; Wu, H.F. Talanta, 2013, **115**, 442–450; (b) Chen, S.; Chen, L.; Wang, J.; Hou, J.; He, Q.; Liu, J.; Wang, J.; Xiong, S.; Yang, G.; Nie, Z. Anal. Chem. 2012, **84**, 10291−10297; (c) Chen, R.; Chen, S.; Xiong, C.; Ding, X.; Chih-Che Wu, C.C.; Chang, H.C.; Xiong, S.; Nie, Z. J. Am. Soc. Mass Spectrom. 2012; **23**, 1454-1460; (d) Abdelhamid, H.N.; Khan, M.S.; Wu, H.F. Anal. Chim. Acta, 2014, **823**, 51–60; (e) Abdelhamid, H.N.; Gopal, J.; Wu, H.F. Anal . Chim.Acta. 2013, **767**, 104–111; (f) Jing Jiao, Ying Zhang, Pengyuan Yang and Haojie Lu, Analyst, 2015, DOI: 10.1039/C4AN01659A
4. (a) Guinan, T.; Kirkbride, P.; Pigou, P.E.; Ronci, M.; Kobus, H.; Voelcker, N.H. Mass Spectrometry Reviews, 2014, DOI 10.1002/mas; (b) Bergman, N.; Denys Shevchenko, D.; Bergquist, J. Anal. Bioanal. Chem. 2014, **406**, 49–61; (c) Chiang, C.K.; Chen, W.-T.; Chang, H. -T. Chem. Soc. Rev. 2011, **40**, 1269–1281; (d) Wu, H.F.; Gopal, J.; Abdelhamid, H.N.; Hasan, N. Proteomics. 2012, **12**, 2949–2961.
5. Novoselov, K. S.; Geim, A. K.; Morozov, S. V.; Jiang, D.; Zhang, Y.; Dubonos, S. V.; Grigorieva, I. V.; Firsov, A. A. Science 2004, **306**, 666−669.

6. (a) Abdelhamid, H.N.; Wu, H.F. Anal.Chim.Acta. 2012, **751**, 94–104; (b) Liu, Q.; Shi, J.B.; Jiang, G.B. TrAC Trends Anal. Chem. 2012, **37**, 1–11.; (c) Kong X, Huang Y; J Nanosci Nanotechnol. 2014, **14**, 4719-32.
7. Abdelhamid, H.N.; Wu, B.S.; Wu, H.F. Talanta. 2014, **126**, 27–37
8. Liu, Q.; Cheng, M.; Jiang, G. Chem. Eur. J. 2013, **19**, 5561 – 5565
9. (a) Sha, Y.; Huang, D.; Zheng, S.; Deng, C. Anal. Methods, 2013, **5**, 4585–4590; (b) Abdelhamid, H.N.; Wu, H.F. J. Mater. Chem. B, 2013, **1**, 3950–3961; (c) Zhao, M.; Deng, C.; Zhang, X. ChemPlusChem 2014, **79**, 359 – 365; (d) Zhao, M.; Deng, C.; Zhang, X. ACS Appl. Mater. Interfaces. 2013, **5**, 13104−13112; (e) Wan, D.; Gao, M.; Wang, Y.; Zhang, P.; Zhang, X. J. Sep. Sci. 2013, **36**, 629–635
10. (a) Li, J.L.; Tang, B.; Yuan, B.; Sun, L.; Wang, X.G. Biomaterials 2013, **34** , 9519-9534; (b) Yang, M.; Yao, J.; Duan, Y. Analyst, 2013, **138**,72–86
11. Yu, X.; Kaixuan Sheng and Gaoquan Shi, Analyst,2014,**139**, 4525–4531
12. Khoshfetrat, S.M.; Mehrgardi , M.A. Analyst, 2014,**139**, 5192-5199
13. Zor, E.; Bingol, H.; Ramanaviciene, A.; Ramanavicius, A.; Ersoz , M. Analyst, 2015, DOI: 10.1039/C4AN01751J
14. Park, J.W.; Park, S.J.; Kwon, O.S.; Lee, C.; Jang, J. Analyst, 2014,**139**, 3852-3855
15. Lin, K.C.; Lai, S.Y.; Chen, S.M. Analyst, 2014,**139**, 3991-3998
16. Bai, Y.; Feng, F.; Zhao, L.; Chen, Z.; Wang, H.; Duan, Y. Analyst, 2014,**139**, 1843-1846
17. Hao, L.; Song, H.; Su, Y.; Lv, Y. Analyst,2014,**139**,764–770
18. Zhen, S.J.; Yu, Y.; Li, C.M.; Huang, C.Z. Analyst 2014, DOI: 10.1039/c4an01433b
19. (a) Lu, J.; Wang, M.; Li, Y.; Deng, C. Nanoscale, 2012, **4**, 1577–1580; (b) Liang, Y.; He, X.; Chen, L.; Zhang, Y. RSC Adv. 2014, **4**, 18132–18135.

20. (a) Guo, Z.; He, L. Anal Bioanal Chem. 2007, **387**,1939–1944; (b) Shanta, S.; Kim, T.; Hong, J.; Lee, J.; Shin, C.; Kim, K.H.; Kim, Y.; Kim, S.; Kim, K. Analyst. 2012, **137**, 5757–5762

21. Chen, T.H.; Yu, C.J.; Tseng, W.L. Nanoscale, 2014, **6**, 1347–1353

22. Kuo, T.R.; Wang, D.Y.; Chiu, Y.C.; Yeh, Y.C.; Chen, W.T.; Chen, C.H.; Chun-Wei Chen, Chang, H.C.; Hu, C.C.; Chen, C.C. Analytica Chimica Acta 2014, **809**, 97– 103

23. Hummers, W.S.; Offeman, R.E. J. Am. Chem. Soc. 1958, **80**, 1339

24. Bagger , N.C.; Tatsumi , H.; Borch , K.; Westh, P. Anal.Biochem. 2014, **447**, 162–168

25. Zhang, H.; Yu, D.; Zhao, Y.; Fan, A. Biosens. Bioelectron. 2014, **61**, 45–50

26. Yang, A.; Zheng, Y.; Long, C.; Chen, H.; Liu, B.; Li, X.; Yuan, J.; Cheng, F. Food Chemistry. 2014, **150**, 73–79

27. Chaudhuri, A.; Chattopadhyay, A. Biochimica et Biophysica Acta. 2014, **1838**, 2078–2086

28. Levinson, S.S.; Elin, R.J.; Yam, L. Clin. Chem.2002, **48**,1131–1132.

29. Li, S.; Gao, Z.; Shao, N. Talanta. 2014, **129**, 86–92

30. Song, Y.; Li, Y.; Liu, Z.; Liu, L.; Wang, X.; Su, X.; Q. Ma, Biosens. Bioelectron 2014, **61**, 9–13

31. Li, S.; Mulloor, J.J.; Wang, L.; Ji, Y.; Mulloor, C.J.; Micic, M.; Orbulescu, J.; Leblanc, R.M. ACS Appl. Mater. Interfaces 2014, **6**, 5704−5712

32. Chen, F.; Gülbakan, B.; Zenobi, R. Chem. Sci., 2013, **4**, 4071–4078

33. Lee, J.W.; Kim, H.I.; Lee, J.W.; Kim, H.I. Analyst, 2014, DOI: 10.1039/C4AN01794C.

34. Dongcheol Choi, Hanall Jeong and Kyuwon Kim, **Analyst**, 2014,**139**, 1331-1333

35. (a) Cherkaoui, A.; Hibbs, J.; Emonet, S.; Tangomo, M.; Girard, M.; Francois, P.; Schrenzel, J. J. Clin. Microbiol., 2010, **48**, 1169–1175 ; (b) Welker, M. Proteomics, 2011, **11**, 3143–3153 ; (c) Sandrin, T.R.; Goldstein, J.E.; Schumaker, S. Mass Spectrom. Rev., 2013, **32**, 188–217 ; (d) Krasny, L.; Hynek, R.; Hochel, I. Int. J. Mass Spectrom., 2013, **353**, 67–7; (e) Wu, H.F.; Gopal, J.; Abdelhamid, H.N.; Hasan, N. Proteomics. 2012, **12**, 2949–2961; (f) Gopal, J.; Abdelhamid, H.N.; Hua, P.Y.; Hui-Fen Wu, H.F. J Mater. Chem. B, 2013, **1**, 2463-2475; (g) Abdelhamid, H.N.; Wu, H.F. J. Mater. Chem. B, 2013, **1**, 3950–3961; (h) Abdelhamid, H.N.; Wu, H.F. J. Mater. Chem. B, 2013, **1**, 6094-6106; (l) Abdelhamid, H.N.; Wu, H.F. Colloids and Surfaces B: Biointerfaces, 2014, 115, 51–60; (m) Abdelhamid, H.N.; Bhaisare, M.; Wu, H.F. Talanta, 2014, **120**, 208–217; (n) Bhaisare, M.L.; Abdelhamid, H.N.; Wu, B.S.; Wu, H.F. J. Mater. Chem. B, 2014, **2**, 4671-4683

36. Nakata, K.; Ichibangase, T.; Saitoh, R.; Ishigai, M.; Imai, K. Analyst, 2014, DOI: 10.1039/c4an01434k

37. Chang Liu, Dongneng Jiang, Guiming Xiang, Linlin Liu, Fei Liu and Xiaoyun Pu, Analyst, 2014,**139**, 5460-5465

38. Qin Tu, Long Pang, Yun Chen, Yanrong Zhang, Rui Zhang, Bingzhang Lu, Jinyi Wang , Analyst 2014,139,105–115

39. (a) Liu, Y.; Li, Y.; Liu, J.Y.; Deng, C.H.; Zhang, X.M. J. Am. Soc. Mass Spectrom., 2011, **22**, 2188–2198; (b) Wu, B.S.; Abdelhamid, H.N.; Wu, H.F. RSC advances, 2014, **4**, 3722-3731.

40. Fagerquist, C.K.; Sultan, O.; Carter, M.Q. J. Am. Soc. Mass Spectrom. 2012, **23**, 2102-2114

41. Toh-Boyo, G.M.; Wulff, S.S.; Basile, F. Anal. Chem. 2012, **84**, 9971−9980.

42. Cohen, S.L.; Chait, B.T. Anal. Chem. 1996, **68**, 31-37.

43. Loo, R.R.O.; Loo, J.A. Anal. Chem. 2007, **79**, 1115-1125.

44. Vargha, M.; Takáts, Z.; Konopka, A.; Nakatsu, C.H. J. Microbiolog. Methods. 2006, **66** , 399–409.

45. Li, P.H.; Huang, S.Y.; Chen, Y.C.; Urban, P.L. RSC Adv. 2013, **3**, 6865–6870.

46. Rana, M.; Balcioglu, M.; Robertson, N._; Yigit, M.V. Analyst,2014,139,714–720

47. Zhang, Z.; Liu, Y.; Ji, X.; Xiang, X.; He, Z. Analyst, 2014,139, 4806-4809; (b) Jing Zhang, Mangjuan Tao and Yan Jin, Analyst, 2014,139, 3455-3459

Table 1. Comparison among the different techniques that were reported for detection and biosening

Anlayte	Probe	Techniques	LOD	Linear Range	Assay time	Ref.
Trypsin	Modified graphene	Chemiluminescent	10 pM	ND	30 mins	[24]
	SA	MADLI-MS	5 pmole	ND	<10 mins	Here
	SA@GO	MALDI-MS	10 fmole	ND	<10 mins	Here
α- lactalbumin	CdSe/ZnS@AB	FLISA	0.1 ng/mL	0.1- 1000 ng/mL	30 mins	[25]
	SA	MADLI-MS	15 pmole	ND	<10 mins	Here
	SA@GO	MALDI-MS	10 fmole	ND	<10 mins	Here
Lysozyme	CdTe (@DNA-LBD	Fluorescence	4.3 nM	8.9–71.2 nM	45 mins	[28]
	CMCS-QDs	Fluorescence	0.031 ng/mL	0.1–1.2 ng/mL	30 mins	[29]
	SA	MADLI-MS	5 pmole	ND	<10 mins	Here
	SA@GO	MALDI-MS	1 fmole	ND	<10 mins	Here
	CILMS	MALDI-MS	4.3×10^{3} cfu/mL	ND	<15 mins	[35n]

S.aureus	SA	MALDI-MS	5×10^4 cfu/mL	ND	<10mins	Here
	SA@GO	MALDI-MS	5×10^3 cfu/mL	ND	<10 mins	Here
P.aeruginosa	CILMS	MALDI-MS	3.2×10^3 cfu/mL	ND	<15 mins	[35n]
	SA	MALDI-MS	3×10^4 cfu/mL	ND	<10mins	Here
	SA@GO	MALDI-MS	4×10^3 cfu/mL	ND	<10 mins	Here

FLISA: fluorescence-linked immunosorbent assay; CMCS-QDs : Carboxymethyl chitosan modified CdTe quantum dots; capped CdTe quantum dots (QDs) conjugated with lysozyme binding DNA (LBD), CdSe/ZnS @AB , monoclonal antibody bioconjugated with CdSe/ZnS @AB quantum dots.